Dihydroartemisinin induces ferroptosis in T cell acute lymphoblastic leukemia cells by downregulating SLC7A11 and activating the ATF4-CHOP signaling pathway

NA TANG[1,2*], XINLING LIU[1*], YONG LIU[1], HAIHUA WANG[1], YAO ZHAO[1], HAIYING WANG[1] and ZHENBO HU[1]

[1]Department of Hematology, Laboratory for Stem Cell and Regenerative Medicine, Affiliated Hospital of Weifang Medical University, Weifang, Shandong 261042, P.R. China; [2]Graduate School, Weifang Medical University, Weifang, Shandong 261053, P.R. China

Received November 27, 2023; Accepted May 2, 2024

DOI: 10.3892/ol.2024.14470

Abstract. The present study aimed to investigate the anti-leukemic effects of dihydroartemisinin (DHA) on T-cell acute lymphoblastic leukemia (T-ALL) cell lines, Jurkat and Molt-4, and the underlying mechanisms. Cell Counting Kit-8 was performed to measure cell viability. Cell apoptosis and cell cycle distribution were assessed by flow cytometry. The expression levels of ATF4 and CHOP mRNA were assessed by reverse transcription-quantitative PCR, while the protein abundance of SLC7A11, GPX4, ATF4 and CHOP was determined by western blotting. Moreover, malondialdehyde, glutathione (GSH) and reactive oxygen species (ROS) assays were used to detect the levels of ferroptosis. The results showed that DHA suppressed T-ALL cell viability *in vitro*, and induced cell cycle arrest at S or G_2/M phase. DHA also induced ROS burst, activated endoplasmic reticulum (ER) stress, disrupted the system Xc^--GSH-GSH peroxidase 4 antioxidant system, and increased lipid peroxide accumulation, resulting in cell death. By contrast, the pharmacological inhibition of ferroptosis alleviated DHA-induced cell death, confirming that DHA induces T-ALL cell death via ferroptosis. Mechanistically, the effect of DHA on ferroptosis was partly mediated by downregulating SLC7A11 and upregulating the ATF4-CHOP signaling pathway, which is associated with ER stress. These results indicated that DHA may induce ferroptosis in T-ALL cell lines and could represent a promising therapeutic agent for treating T-ALL.

Correspondence to: Dr Zhenbo Hu or Dr Haiying Wang, Department of Hematology, Laboratory for Stem Cell and Regenerative Medicine, Affiliated Hospital of Weifang Medical University, 2428 Yuhe Road, Weifang, Shandong 261042, P.R. China
E-mail: huzhenbo@sdsmu.edu.cn
E-mail: wanghaiying1121@126.com

*Contributed equally

Key words: dihydroartemisinin, T-cell acute lymphoblastic leukemia, ferroptosis, endoplasmic reticulum stress

Introduction

T-cell acute lymphoblastic leukemia (T-ALL) is a disease characterized by the uncontrolled proliferation of mature or immature T cells (1). T-ALL is more common in adults than in children, although the incidence starts to diminish with age after 10 years old. Notably, T-ALL accounts for 15% of childhood and 25% of adult cases of ALL (2). The outcomes of patients with T-ALL have improved as novel therapies have been identified and existing therapies have improved; however, the 5-year survival rate has remained poor, with event-free and overall survival rates of <25% for relapsed disease (3). In addition, treatment resistance, disease recurrence, treatment-related deaths and long-term harmful side effects of chemotherapy in cancer survivors remain serious issues that need to be addressed. Therefore, discovering more effective but less toxic strategies for treating T-ALL is a priority.

According to statistics, >50% of modern clinical antitumor drugs are directly or indirectly derived from natural products and their derivatives (4). Dihydroartemisinin (DHA; Fig. 1A), a water-soluble semi-synthetic derivative of artemisinin, is a sesquiterpene lactone with a peroxide moiety that has long been an essential component of anti-malarial therapy (5). Increasing evidence has demonstrated that DHA possesses multiple pharmacological actions, including, but not limited to, anti-viral, anti-inflammatory and anticancer effects (6). Based on the safety profile of DHA, a number of studies have assessed the antitumor effects of DHA on glioma (7), liver cancer (8) and breast malignancies (9).

DHA has been shown to possess a number of anti-tumor mechanisms, including induction of apoptosis- and autophagy-mediated cell death, adjustment of the tumor immune microenvironment, and suppression of metastasis and angiogenesis (10,11). DHA has also been reported to suppress the invasion and migration of bladder cancer cells via the downregulation of histone demethylase KDM3A expression and induction of p21 expression (12). The role of DHA in inducing apoptosis in T-ALL cells was first reported by Sun *et al* (13). A recent study has revealed that the anticancer effects of DHA are highly reliant on the cleavage of the endoperoxide bridge within its molecular structure and subsequent reactive oxygen species (ROS) generation (14). In addition, the

selective cytotoxic effects of DHA on some cancer cells are associated with ferroptosis, which is a non-apoptotic type of cell death (15,16).

Ferroptosis is characterized by the accumulation of intracellular soluble and lipid ROS, which can be counteracted by the glutathione (GSH)-dependent activity of the GSH peroxidase 4 (GPX4) enzyme (17). System Xc^-, also named cystine-glutamate antiporter, is composed of the light chain SLC7A11 (also commonly known as xCT) linked via a disulfide bridge to the heavy chain SLC3A2. It is an essential intracellular antioxidant element and functions as a regulator for GSH synthesis (18). Suppressing system Xc^- triggers an excess of ROS and lipid peroxidation, ultimately resulting in cell death and diseases such as neurodegenerative and cardiovascular diseases (19-21). In addition, Dixon *et al* (22) proposed that the inhibition of system Xc^- leads to endoplasmic reticulum (ER) stress, evidenced by transcriptional upregulation of genes associated with the ER stress response, and posited a close correlation between ER stress elevation and erastin-induced ferroptosis.

To the best of our knowledge, no study has determined whether DHA can affect ferroptosis in T-ALL cells. Therefore, the present study aimed to investigate the regulatory mechanisms of DHA for ferroptosis in T-ALL, and to develop novel approaches for treating T-ALL.

Materials and methods

Reagents and antibodies. DHA and ferrostatin-1 (Fer-1), purchased from Glpbio Technology, Inc., were dissolved in DMSO and stored at -20˚C. In all experiments, the final DMSO concentration was 0.1% (v/v), and DMSO alone had no demonstrable effect on cultured cells. DMSO (0.1%) served as the vehicle control. RPMI-1640 medium, fetal bovine serum (FBS), penicillin (5,000 U/ml), streptomycin (5,000 mg/ml) and SparkZol reagent were purchased from Shandong Sparkjade Biotechnology Co., Ltd. The propidium iodide (PI)/RNase staining buffer and the fluorescein isothiocyanate (FITC) Annexin V apoptosis detection kit were purchased from BD Biosciences. Anti-SLC7A11/xCT antibody [cat. no. ab175186; 1:2,000 for western blotting (WB)] was purchased from Abcam; anti-GPX4 antibody (cat. no. 67763-1-Ig; 1:1,000 for WB) and anti-GAPDH antibody (cat. no. 60004-1-Ig; 1:10,000 for WB) were purchased from Wuhan Sanying Biotechnology; anti-ATF4 antibody (cat. no. A18687; 1:1,000 for WB) and anti-CHOP antibody (cat. no. A21902; 1:1,000 for WB) were purchased from ABclonal Biotech Co., Ltd. HRP Goat Anti-Mouse IgG (cat. no. AS003; 1:10,000 for WB) and HRP Goat Anti-Rabbit IgG (cat. no. AS014; 1:10,000 for WB) were also purchased from ABclonal Biotech Co., Ltd.

Cell lines and cell culture. Jurkat T-ALL cells were acquired from Leibniz Institute DSMZ-German Collection of Microorganisms and Cell Cultures GmbH, and Molt-4 T-ALL cells were purchased from The Cell Bank of Type Culture Collection of The Chinese Academy of Sciences. Both cell lines were cultured in RPMI-1640 medium supplemented with 10% FBS and 1% penicillin-streptomycin solution. Cells were cultured in a humidified incubator at 37˚C with 5% CO_2.

Isolation of peripheral blood mononuclear cells (PBMCs) from cord blood. Cord blood samples were collected from three healthy mothers who gave birth at the Affiliated Hospital of Weifang Medical University (Weifang, China) in March 2024 after providing written informed consent. Briefly, ~20 ml cord blood was collected from each sample into EDTA anticoagulant tubes and diluted with 20 ml PBS. Subsequently, 20 ml diluted cord blood was layered onto 15 ml Ficoll-Paque (Beijing Solarbio Science & Technology Co., Ltd.) in a 50-ml conical tube and centrifuged at 400 x g for 30 min at 18˚C. The PBMC fraction was then transferred to another tube and washed twice with PBS. Cell viability was required to exceed 90% of total cells determined by trypan blue assay for each sample. In brief, the cell suspension was mixed with 0.4% Trypan Blue solution (cat. no. 93595, Sigma-Aldrich, Beijing, China) in a 9:1 ratio, mix gently and allow to stain for 3-5 min. The stained cell suspension was loaded onto the hemocytometer, the number of viable (unstained, clear) and non-viable (stained, blue) cells were counted in the gridded area of the hemocytometer using a microscope. Cell viability was calculated as a percentage using the formula: Viability=(Number of viable cells/Total number of cells) x100%.

Cell viability and proliferation assay. To evaluate the viability and proliferation of T-ALL cells, the Cell Counting Kit-8 (CCK-8; Beijing Solarbio Science & Technology Co., Ltd.) was used. Jurkat and Molt-4 cells were seeded in 96-well plates at a density of 5,000 cells/well and were treated with DHA at the indicated concentrations (0, 2.5, 5, 10 and 20 μM for Molt-4; 0, 5, 10, 20 and 40 μM for Jurkat) for 24, 48 and 72 h at 37˚C. Cytotoxic effects of DHA on PBMCs isolated from cord blood were evaluated PBMCs were seeded into 96-well plates ($1x10^5$ cells per well) and treated with various DHA concentrations (0, 5, 10, 20 and 40 μM) for 24, 48 and 72 h at 37˚C. Furthermore, Jurkat and Molt-4 cell lines were treated with DHA (10 μM), Fer-1 (1 μM) or both for 48 h at 37˚C. Following the treatment, 10 μl CCK-8 solution was added to each well and incubated for 3 h, according to the manufacturer's protocol. The optical density (OD) was measured at a wavelength of 450 nm using a microplate reader (Multiskan GO; Thermo Fisher Scientific, Inc.). Cell viability was calculated as the OD value of treated cells/OD value of control cells. The IC_{50} for each cell line was calculated based on the OD value corresponding to 50% inhibition by DHA.

Cell apoptosis assay. Jurkat and Molt-4 cells were plated in 6-well plates at a density of $5x10^5$ cells/well and were treated with DHA (0, 5, 10, and 20 μM) for 48 h at 37˚C. In addition, cells ($5x10^5$/ml) were treated with DHA (10 μM) in the presence or absence of Fer-1 (1 μM) for 48 h at 37˚C. Subsequently, the cells were collected, washed twice in cold 1X PBS, and resuspended in 300 μl binding buffer containing 5 μl PI and 5 μl Annexin V-FITC for 30 min in the dark at room temperature. The percentage of apoptotic cells was determined using a Flow Cytometer (DxFLEX; Beckman Coulter, Biotechnology (Suzhou) Co., Ltd.). The data were analyzed using CytExpert software for DxFLEX (version 2.0.0.283, Beckman Coulter, Inc.) and FlowJo software (version 10.8.1, Becton, Dickinson & Company).

Cell cycle analysis. A PI/RNase Staining Solution kit was used to assess cell cycle distribution. After 48 h of treatment at 37˚C with various doses of DHA (Jurkat cells: 5, 10, and 20 μM; Molt-4 cells: 2.5, 5, and 10 μM) or vehicle control, both cells were then harvested and washed twice with pre-cooled PBS. The cells were then fixed with 70% cold ethanol at -20˚C overnight. Subsequently, the cells were then stained with 500 μl PI/RNase buffer at room temperature in the dark for 15 min, according to the manufacturer's instructions. The cell cycle was examined using flow cytometry (DxFLEX; Beckman Coulter, Inc.) and data were analyzed using FlowJo software (version 10.8.1; Becton, Dickinson & Company).

ROS analysis. ROS levels in cells were measured using 2',7'-dichlorofluorescin diacetate (DCFH-DA; Beijing Solarbio Science & Technology Co., Ltd.). Jurkat and Molt-4 cells were seeded in 6-well plates at a density of $1x10^6$ cells/well. The cells were treated with DHA at the indicated concentrations (0, 5, 10, 20, and 40 μM for Jurkat; 0, 2.5, 5, 10, and 20 μM for Molt-4) for 48 h at 37˚C. Furthermore, both cell lines were treated with DHA (10 μM), Fer-1 (1 μM), or a combination of both for 48 h at 37˚C. After the indicated treatments, cells were harvested and washed twice with PBS and suspended in serum-free culture medium containing DCFH-DA at a final concentration of 10 μmol/l at 37˚C for 30 min. Finally, fluorescence intensity was determined by flow cytometry (DxFLEX; Beckman Coulter, Biotechnology (Suzhou) Co., Ltd.) and the results were analyzed using FlowJo software.

GSH and malondialdehyde (MDA) assays. Intracellular GSH levels were detected using a Reduced GSH Content Assay Kit (Beijing Solarbio Science & Technology Co., Ltd.). MDA, as an end product of lipid peroxidation, was evaluated using the MDA Content Assay Kit (Beijing Solarbio Science & Technology Co., Ltd.). All assays were performed in strict accordance with the kit protocol.

WB. Jurkat and Molt-4 ($5x10^5$ cells/per well) were cultured in 6-well plates with 10, 20, 40 μM and 5, 10, 20 μM DHA for 48 h at 37˚C, respectively. Pretreated cells were lysed on ice with RIPA buffer (Shandong Sparkjade Biotechnology Co., Ltd.) containing 0.1% protease inhibitor and 1% phenylmethylsulfonyl fluoride. The soluble fraction was isolated by centrifugation at 12,000 x g for 10 min at 4˚C, and the supernatant was transferred to a new tube. Subsequently, a BCA kit was used to determine protein concentration. Equal amounts of protein from each sample (20 μg) were separated by SDS-PAGE on 12.5 or 15% gels, and were then transferred to 0.22-μm polyvinylidene fluoride membranes, which were sealed with 5% nonfat dry milk in Tris-buffered saline-0.1% Tween-20 (TBST) for 2 h at room temperature. The membranes were then incubated overnight at 4˚C with primary antibodies against GAPDH, SLC7A11, GPX4, ATF4 and CHOP, followed by incubation with secondary antibodies for 1 h at room temperature, before being washed with TBST three times. Finally, an Ultra High Sensitivity ECL Kit (cat. no. GK10008, Glpbio Technology) was used to visualize the proteins on the membranes using an Amersham Imager 600 (GE Healthcare Bio-Sciences), and Image J software version 1.53t (National Institutes of Health) was subsequently employed for semi-quantitative analysis of the obtained images.

Reverse transcription-quantitative PCR (RT-qPCR). Total RNA was extracted from the control and DHA-treated, Fer-1-treated, and combination-treated Jurkat and Molt-4 cells using SparkZol reagent and was quantified using an ultra-micro spectrophotometer (NanoDrop OneC; Thermo Fisher Scientific, Inc.). According to manufacturer's protocol, RNA (1 μg) was reverse transcribed into cDNA using the Evo M-MLV RT Premix (Hunan Aikeru Bioengineering Co., Ltd.). The mRNA expression levels of ATF4, CHOP and GAPDH were measured by qPCR in 96-well plates with cDNA as the template using a 7500 Fast Real-Time PCR system (Applied Biosystems; Thermo Fisher Scientific, Inc.) and 2X SYBR® Green Premix Pro TaqHS qPCR Kit (Hunan Aikeru Bioengineering Co., Ltd.). The reaction conditions for amplification were set according to the manufacturer's instructions: Initial denaturation, 95˚C for 30 sec, followed by 40 cycles of denaturation (95˚C for 10 sec), annealing (55˚C for 20 sec) and extension (72˚C for 30 sec). The relative gene expression levels were calculated using the $2^{-\Delta\Delta Cq}$ method (23). GAPDH was used as the internal control. The primer sequences were as follows: ATF4, forward 5'-AAGCCTAGGTCTCTTAGATG-3', reverse 5'-TTCCAGGTCATCTATACCCA-3'; CHOP, forward 5'-GGAAACAGAGTGGTCATTCCC-3', reverse 5'-CTGCTTGAGCCGTTCATTCTC-3'; and GAPDH, forward 5'-ACAACTTTGGTATCGTGGAAGG-3' and reverse 5'-GCCATCACGCCACAGTTTC-3'.

Statistical analysis. Statistical analysis was performed using GraphPad Prism 8.0 software (Dotmatics). All data are presented as the mean ± SD and experiments were performed in triplicate. The differences between two groups were determined using the unpaired two-tailed Student's t-test. Comparisons among multiple groups were analyzed by one-way ANOVA followed by Tukey's multiple comparisons test. $P<0.05$ was considered to indicate a statistically significant difference.

Results

DHA treatment suppresses T-ALL cell viability in vitro. To assess whether DHA can inhibit the proliferation of T-ALL cells *in vitro*, the CCK-8 assay was used to detect the effects of DHA on the viability of T-ALL cell lines. Jurkat and Molt-4 cells were treated with DHA at various concentrations, ranging from 0 to 40 μM for 24, 48 and 72 h. As demonstrated in Fig. 1B, the results showed that at the same dosages used to treat the T-ALL cell lines Jurkat and Molt-4, DHA displayed minimum toxicity in PBMCs. Compared with in the control groups, the viability of the two T-ALL cell lines after DHA treatment was significantly decreased in a time- and dose-dependent manner. DHA at 2.5 and 5 μM significantly reduced the viability of Molt-4 and Jurkat cells at 24 h compared to the control group, respectively. When the DHA concentration was ≥20 μM, DHA exhibited a certain level of toxicity towards PBMCs. However, in comparison to PBMCs, 20 μM DHA was more inclined to induce cell death in T-ALL cells. After 48 h of incubation, the IC_{50} of DHA was 8.324 μM

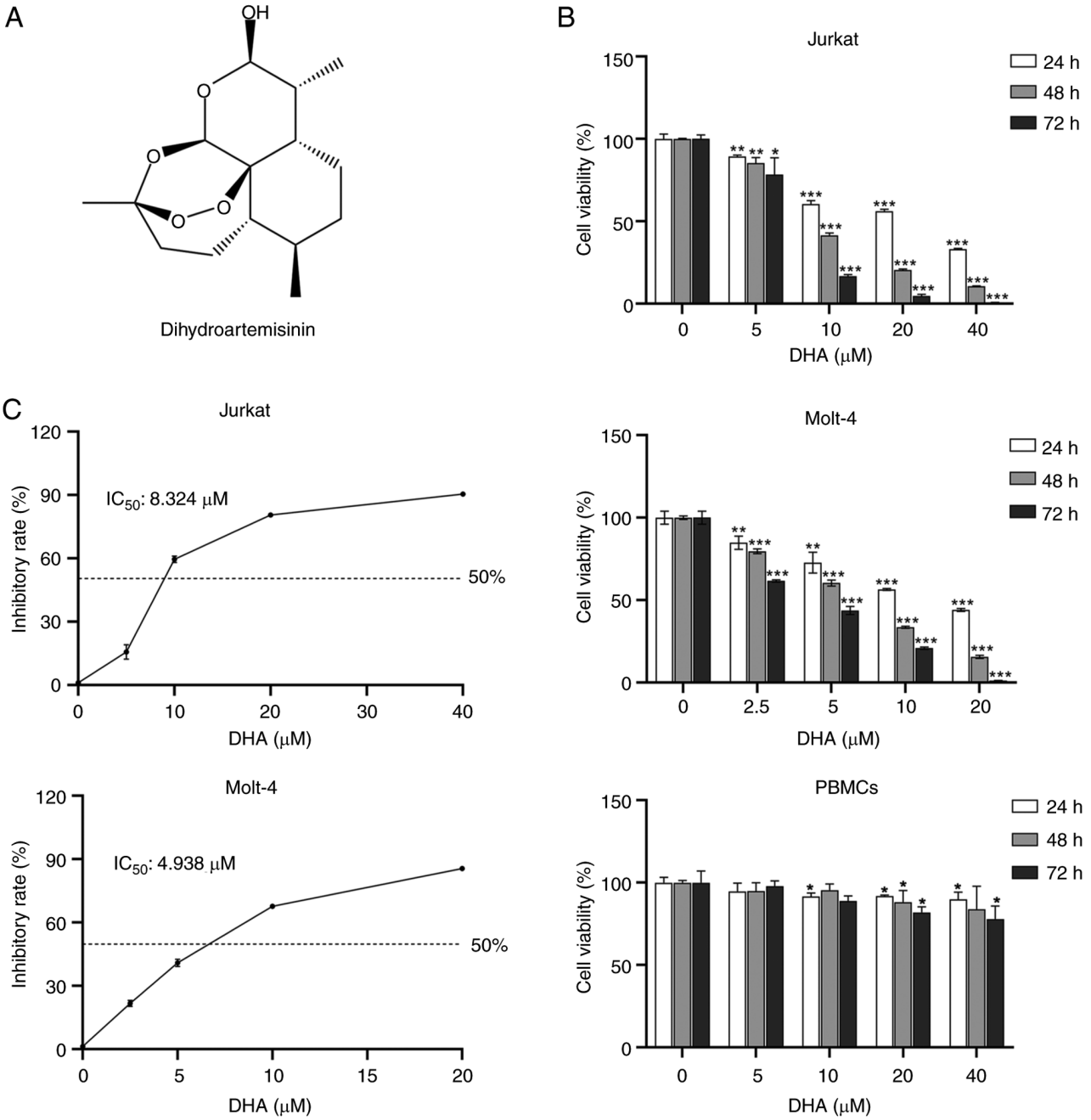

Figure 1. DHA inhibits the viability of T-ALL cells. (A) Chemical structure of DHA. (B) Cell viability was assessed using Cell Counting Kit-8 after treatment of Jurkat cells, Molt-4 cells and PBMCs with DHA at 24, 48 and 72 h. (C) IC_{50} values of DHA at 48 h in T-ALL cell lines. *P<0.05, **P<0.01, ***P<0.001 vs. 0 μM DHA. DHA, dihydroartemisinin; PBMCs, peripheral blood mononuclear cells; T-ALL, T-cell acute lymphoblastic leukemia.

(Jurkat) and 4.938 μM (Molt-4) (Fig. 1C). Molt-4 cells were more sensitive than Jurkat cells to DHA. For the selection of DHA doses in subsequent experiments, the concentrations were based on preliminary CCK-8 experiments as specified above. These experiments helped determine the appropriate range of DHA concentrations that would not cause excessive cell death while still eliciting a biological response.

DHA induces apoptosis in T-ALL cells. The present study subsequently evaluated the effects of DHA treatment on the induction of cell death in T-ALL cells. Jurkat and Molt-4 cells were treated with different doses of DHA (5, 10 and 20 μM) for 48 h, and cell death was detected by FITC-Annexin V staining. As depicted in Fig. 2A and B, following a 48-h exposure of the two T-ALL cell lines to DHA, there was a dose-dependent increase in cell death. Cells treated with DHA were predominantly clustered in the right upper quadrant of the scatter plots (Annexin V- and PI-positive cells), indicating late apoptotic cells. In the presence of 10 μM DHA, the proportion of early and late apoptotic Molt-4 and Jurkat cells were 28.41±0.67 and 16.33±0.93%, respectively. Molt-4 cells treated with 20 μM DHA exhibited a 52.6% proportion of late apoptotic or dead cells. However, the proportion of cells in the right upper quadrant decreased after Fer-1 treatment compared with that in the DHA group. The proportion of late apoptotic or dead cells in the DHA + Fer-1-treated Jurkat

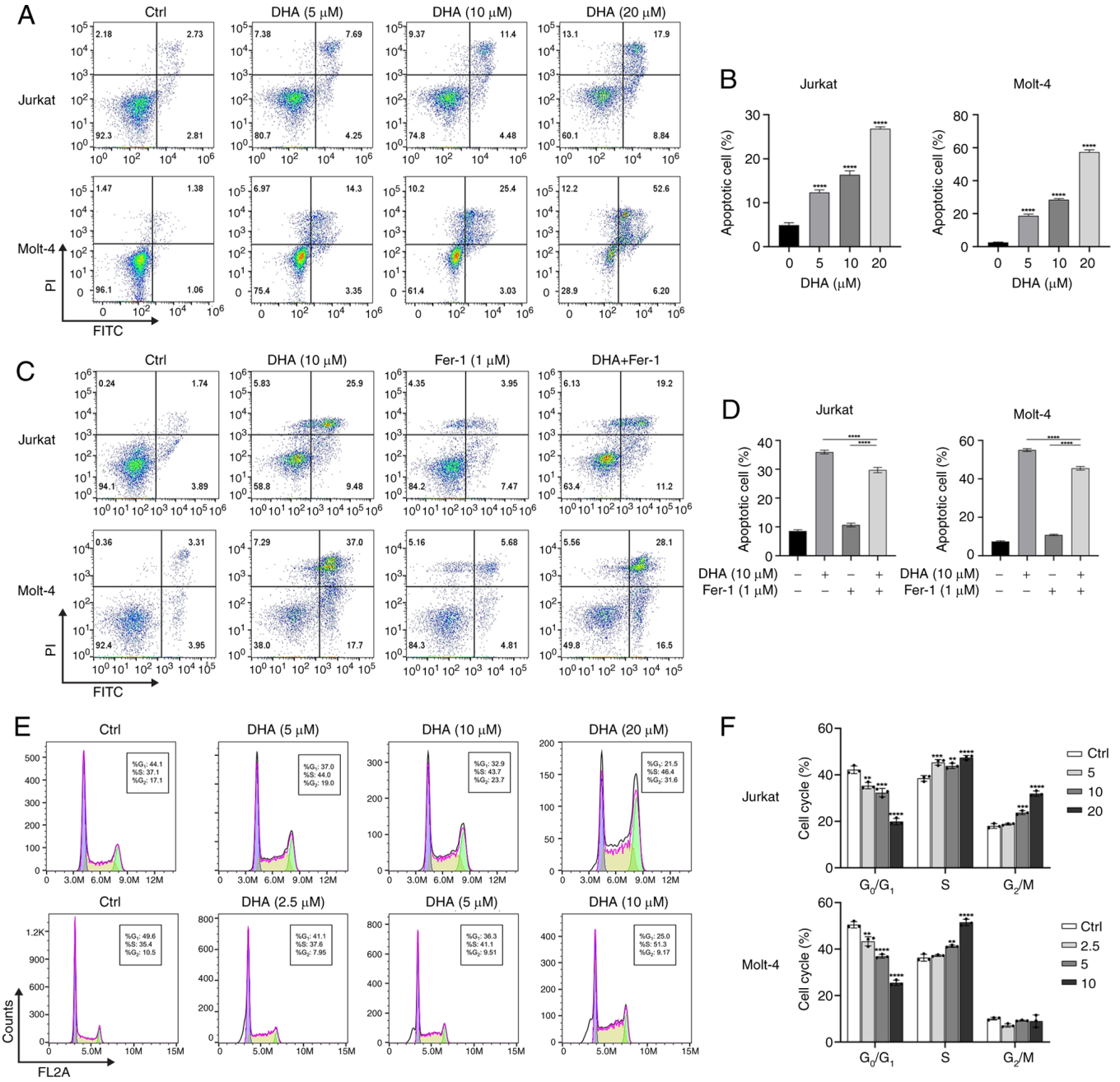

Figure 2. Changes in cell cycle progression and cell death induced by DHA in Jurkat and Molt-4 cells. (A) Cells were treated with DHA (0, 5, 10 and 20 μM) for 48 h, followed by Annexin V/FITC and PI double staining, and flow cytometric analysis of apoptosis. (B) Quantification of the number of apoptotic cells in (A). (C) Flow cytometric analysis of Annexin V/FITC and PI-stained T-cell acute lymphoblastic leukemia cell lines incubated with DHA (10 μM) for 48 h with or without Fer-1 (1 μM). (D) Quantification of the number of dead cells in (C). (E) Jurkat cells were treated with DHA (5, 10 and 20 μM) and Molt-4 cells were treated with DHA (2.5, 5 and 10 μM) for 48 h, followed by PI staining and flow cytometric analysis of cell cycle distribution. (F) Cell cycle distribution analysis of (E). **P<0.01, ***P<0.001, ****P<0.0001 vs. 0 μM DHA. DHA, dihydroartemisinin; Fer-1, ferrostatin-1; FITC, fluorescein isothiocyanate; PI, propidium iodide.

and Molt-4 cells decreased by 6.7 and 8.9%, respectively, compared with the DHA-treated group (Fig. 2C and D). Initially, the selection of DHA concentrations was guided by the CCK-8 data, focusing on those concentrations that were close to the IC_{50}. Notably, when treated with 20 μM DHA, there was a marked increase in cell apoptosis, particularly in Molt-4 cells, where the apoptosis rate exceeded 50%. In order to ensure comparability between Jurkat and Molt-4 cells, the present study ultimately opted for a DHA concentration of 10 μM when performing co-treatments with Fer-1. The present findings suggested that DHA can induce apoptosis in T-ALL cells; however, the results of Annexin V/PI staining pointed towards a mechanism that may be involved in ferroptosis other than apoptosis.

DHA induces cycle arrest in T-ALL cell lines. To determine whether the decreased viability of DHA-treated T-ALL cells was attributable to the induction of cell cycle arrest, flow cytometry was applied to analyze the effect of DHA on cell cycle distribution. By comparing the cell proportions at each phase in response to different doses of DHA, it was revealed that Jurkat cells began to accumulate in the S phase and G_2/M

phase in a dose-dependent manner following treatment with DHA for 48 h. In Molt-4 cells, the proportion of cells in G_0/G_1 phase gradually decreased from 49.6 to 25%, while the percentage of cells in the S phase increased from 35.4 to 51.3%, with increasing concentrations of DHA (Fig. 2E and F). Therefore, DHA may facilitate the transition of T-ALL cells from the G_1 phase to S phase, subsequently inducing cell cycle arrest in the S and G_2/M phases, weakening their proliferative capacity and reducing cell viability.

The present study also performed the experiments after prolonged treatment of Jurkat and Molt-4 cells with DHA for 72 h. The results showed that DHA arrested the Jurkat cell cycle in S and G_2/M phases, and the Molt-4 cell cycle in G_0/G_1 phase (Fig. S1B), which may hinder cell proliferation and was positively associated with the results of apoptosis analysis. For example, when Jurkat cells were treated with 10 μM DHA for 72 h, the cell cycle was arrested in S and G2/M phases, and apoptotic cells increased by 35.84% (Fig. S1A). As Molt-4 cells exhibited higher sensitivity to DHA, prolonged treatment of the Molt-4 cells with DHA for 72 h resulted in the majority of the cells exiting the cell cycle and ceasing proliferation, thus resulting in an increased proportion of cells in the G_0/G_1 phase. These results suggested that the distinct mechanism for cell cycle arrest serves a crucial role in ensuring an appropriate response to DNA damage over time.

DHA induces ferroptosis in T-ALL cells. Ferroptosis is a type of programmed cell death driven by the accumulation of ROS and lipid peroxides closely related to oxidative stress and cystine metabolism (17). To investigate whether ferroptosis is associated with DHA-induced cell death in T-ALL cells, cytoplasmic ROS was quantified by flow cytometry using DCFH-DA probe staining. As shown in Fig. 3A, cytoplasmic ROS levels were markedly increased in Jurkat and Molt-4 cells after DHA treatment. Following treatment with 10 and 20 μM DHA, respectively, the FITC-A subsets of Jurkat cells were 15.0 and 35.4, and those of Molt-4 cells were 38.0 and 55.7, which were consistent with the previous results, indicating the higher sensitivity of Molt-4 cells to DHA. The present study subsequently examined the protein expression levels of SLC7A11 and GPX4 after 48 h of treatment with different doses of DHA. Compared with those in the control group, the expression levels of SLC7A11 and GPX4 were significantly downregulated in the DHA-treated groups (Jurkat cells with 20, 40 μM DHA; Molt-4 cells with 10, 20 μM DHA), as indicated in Fig. 3B. A previous study revealed that lipid peroxides are typically removed catalytically by the antioxidant enzyme GPX4, a process that requires GSH as a cofactor (24). Therefore, the present study examined MDA and GSH levels in the T-ALL cells treated with DHA. As shown in Fig. 3C, in response to treatment with 5 μM DHA, there was no discernible impact on the MDA content in either Jurkat or Molt-4 cells. At 10 μM DHA, the MDA content in Jurkat and Molt-4 cells was significantly increased compared with that in the control group. In response to 20 μM DHA, the MDA content doubled in both Jurkat and Molt-4 cells compared to the control group, indicating prolonged oxidative stress. Similarly, DHA administration reduced GSH levels in T-ALL cells in a dose-dependent manner compared with in the control cells, indicating an impaired antioxidative response, and the GSH content was decreased even in response to a low concentration of DHA (5 μM) (Fig. 3D). The effects of 40 μM DHA on MDA and GSH in Jurkat and Molt-4 cells are not shown because not enough cells obtained following high dose DHA treatment. These results indicated that DHA may trigger ferroptosis in T-ALL cells.

Fer-1 partially attenuates the ferroptosis of T-ALL cells induced by DHA. Fer-1, a specific inhibitor of ferroptosis, has been reported to inhibit lipid peroxidation, thereby protecting cells from lipid peroxidation-induced cellular damage (25). To further assess the effect of DHA on the regulation of ferroptosis, Fer-1 was applied as a ferroptosis inhibitor in the present study. The results revealed that the combined treatment of DHA and Fer-1 inhibited viability compared to the control group; however, cell viability was higher in the DHA + Fer-1 group than in the DHA alone group (Fig. 4A). In addition, the expression levels of SLC7A11 and GPX4 were upregulated in the DHA + Fer-1 group compared with those in the DHA group, suggesting that Fer-1 limited DHA-induced damage to the antioxidant system (Fig. 4B). Subsequently, the effects of Fer-1 pretreatment on ROS, MDA and GSH levels after DHA treatment were examined. As shown in Fig. 4C-E, Fer-1 attenuated the increase in ROS and MDA levels, and rescued the DHA-induced reduction in GSH. These results suggested a rescue role of Fer-1 in DHA-induced cell injury by blocking ferroptosis. The results of WB indicated that there were no statistically significant differences in protein expression levels of SLC7A11, GPX4, ATF4, and CHOP between Jurkat cells treated with 5 and 10 μM DHA (Figs. 3B and 5B). Similarly, Molt-4 cells treated with 2.5 μM DHA did not exhibit significant differences in protein expression of SLC7A11, GPX4, ATF4, and CHOP compared with those treated with 5 μM DHA (Figs. 3B and 5B). Therefore, 10 μM for Jurkat cells and 5 μM for Molt-4 cells were selected as the minimum concentrations for further WB experiments. In the fer-1 rescue experiment, both cell lines were treated with 10 μM of DHA, as shown in Figs. 4B and 5D.

DHA upregulates the expression of ER stress-related genes. Boelens *et al* (26) studied ER stress in cells using a synthesized cytotoxic artemisinin compound conjugated with a fluorescent dansyl moiety, and revealed that the ER is the main site of its accumulation by organelle-specific dye co-localization. ER stress can be triggered by anticancer chemicals, including pro-ferroptotic reagents such as erastin (27). Based on the results of previous study (22), the present study examined the transcription of ER stress-related genes. The results demonstrated that DHA, an emerging inducer of ferroptosis, induced ER stress in T-ALL cells, as shown by elevated mRNA expression levels of ATF4 and CHOP (Fig. 5A). Compared with in the control group treated with DMSO, DHA also upregulated the protein expression levels of ATF4 and CHOP in a dose dependent manner in T-ALL cells (Fig. 5B). The present study further investigated the effect of DHA with or without Fer-1 on the expression levels of ATF4 and CHOP in Jurakt

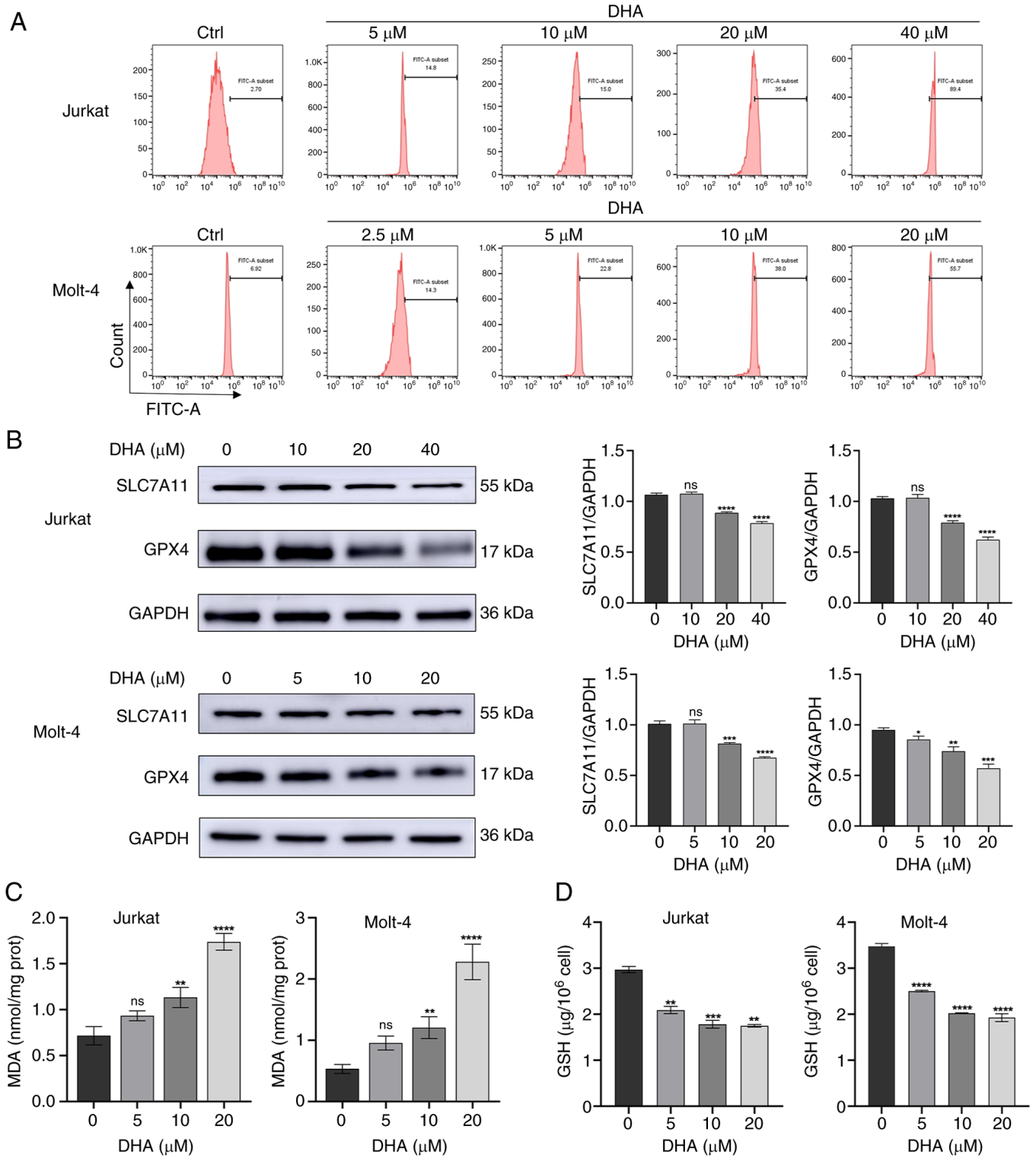

Figure 3. DHA induces ferroptosis in T-ALL cell lines. (A) Jurkat and Molt-4 cells were treated with DHA for 48 h, and cell ROS levels were measured using flow cytometry. (B) Jurkat and Molt-4 cells were treated with DHA for 48 h, and western blotting was used to detect the protein expression levels of SLC7A11 and GPX4 in T-ALL cells. (C) MDA and (D) GSH levels were determined in T-ALL cells exposed to 5, 10 or 20 μM DHA. All the data are representative of three independent experiments. *P<0.05, **P<0.01, ***P<0.001, ****P<0.0001 vs. 0 μM DHA. DHA, dihydroartemisinin; FITC, fluorescein isothiocyanate; GPX4, glutathione peroxidase 4; MDA, malondialdehyde; ns, no significance; T-ALL, T-cell acute lymphoblastic leukemia.

and Molt-4 cells. As expected, the enhancement induced by DHA in Jurkat and Molt-4 cells was attenuated by Fer-1 co-treatment (Fig. 5C and D). These results suggested that ER stress may serve an important role in DHA-induced ferroptosis.

Discussion

The present study investigated the antitumor effect of DHA on T-ALL cells and identified the mechanisms involved. The results demonstrated that DHA significantly decreased

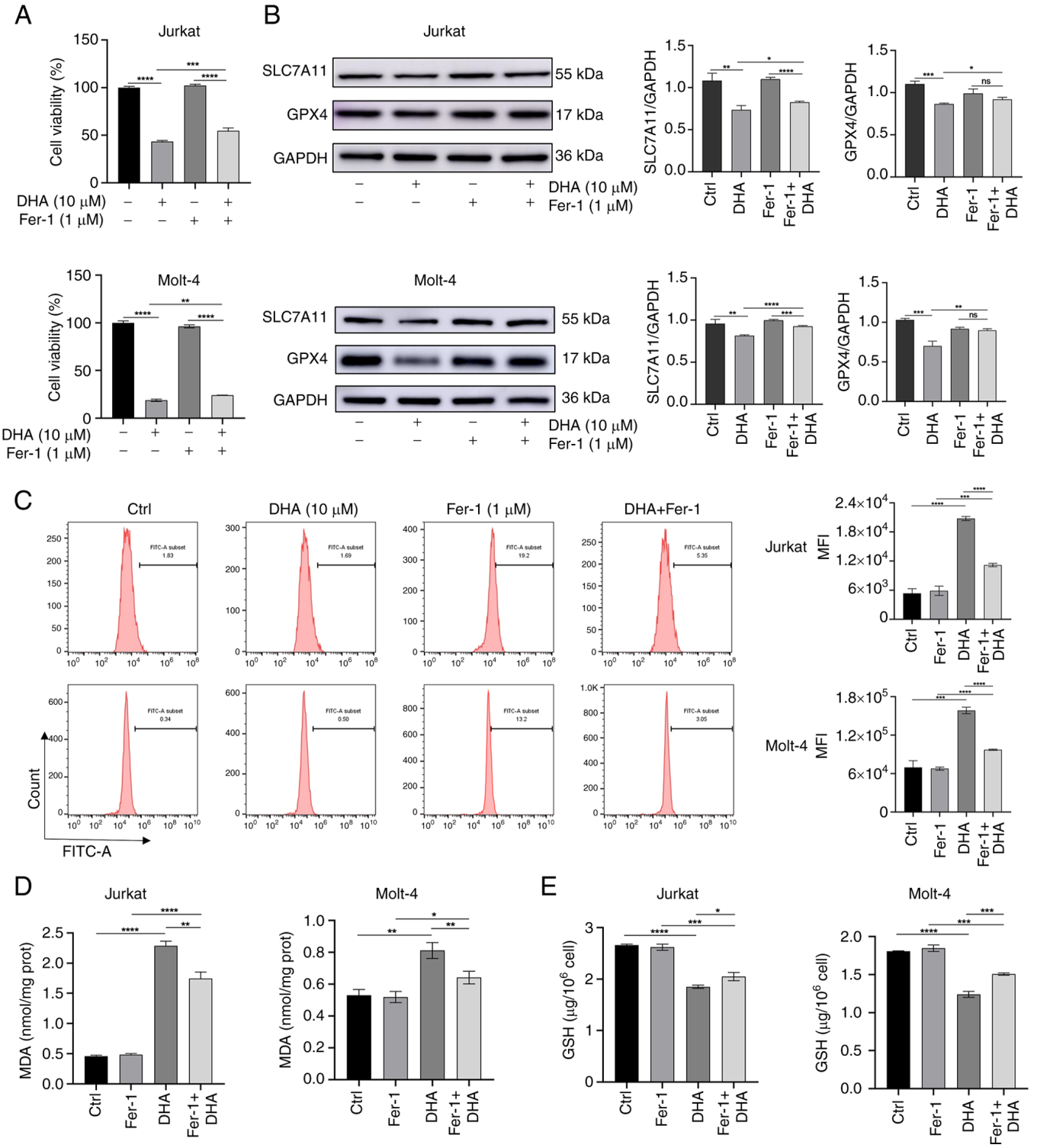

Figure 4. Inhibition of ferroptosis can prevent DHA-induced T-ALL cell death. T-ALL cells were treated with 1 μM Fer-1 and 10 μM DHA for 48 h. (A) Cell Counting Kit-8 was used to assess the viability of T-ALL cells. (B) Western blot analysis measured the protein expression levels of SLC7A11 and GPX4 in different groups of T-ALL cells, with histograms constructed based on their respective relative grayscale values. (C) ROS levels in cells were measured using flow cytometry, followed by assessment of MFI. (D) MDA content was measured. (E) GSH content was measured using a GSH assay kit. *P<0.05, **P<0.01, ***P<0.001, ****P<0.0001. DHA, dihydroartemisinin; Fer-1, ferrostatin-1; FITC, fluorescein isothiocyanate; GPX4, glutathione peroxidase 4; MDA, malondialdehyde; MFI, mean fluorescence intensity; ns, no significance; T-ALL, T-cell acute lymphoblastic leukemia.

T-ALL cell viability, and induced cell cycle arrest at S or G_2/M phase and apoptosis. Furthermore, in T-ALL cells treated with DHA, ferroptosis was markedly induced, as evidenced by elevated levels of MDA and ROS, coupled with decreased GSH levels. Additionally, DHA triggered a significant ER stress response in T-ALL cells. Notably, Fer-1 administration partially recovered the viability of T-ALL cells, enhancing the protein expression levels of SLC7A11 and GPX4, while lowering those of ATF4 and CHOP. These results further suggested the critical role of ferroptosis

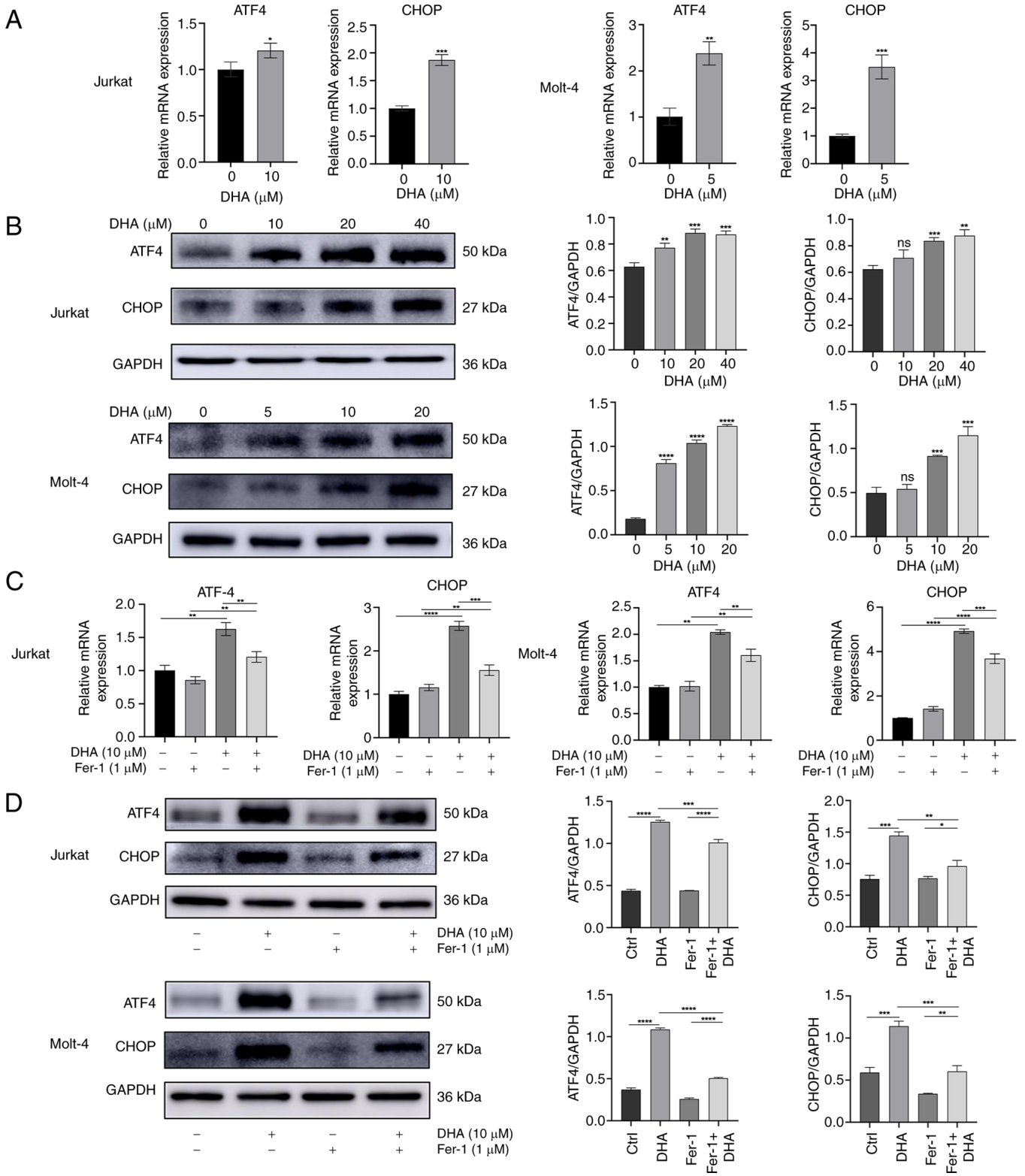

Figure 5. DHA upregulates the expression of ER stress-related genes. (A) Jurkat and Molt-4 cells were cultured in 10 and 5 μM DHA for 48 h, respectively. RT-qPCR was performed to measure the mRNA expression levels of ATF4 and CHOP. (B) Jurkat and Molt-4 cells were cultured in DHA for 48 h. The protein expression levels of ATF4 and CHOP were assessed via western blot analysis, followed by the generation of associated grayscale histograms. The T-cell acute lymphoblastic leukemia cells were treated with 1 μM Fer-1 and 10 μM DHA for 48 h. (C) mRNA expression levels of ATF4 and CHOP were assessed by RT-qPCR. (D) Protein expression levels of ATF4 and CHOP were measured by western blotting, with histograms constructed based on relative grayscale values. *P<0.05, **P<0.01, ***P<0.001, ****P<0.0001 vs. 0 μM DHA or as indicated. DHA, dihydroartemisinin; Fer-1, ferrostatin-1; ns, no significance; RT-qPCR, reverse transcription-quantitative PCR.

in the suppressive effects of DHA on T-ALL biological functions, whereby DHA triggers ferroptosis in T-ALL cells by inhibiting SLC7A11 expression and activating the ATF4-CHOP signaling pathway (Fig. 6).

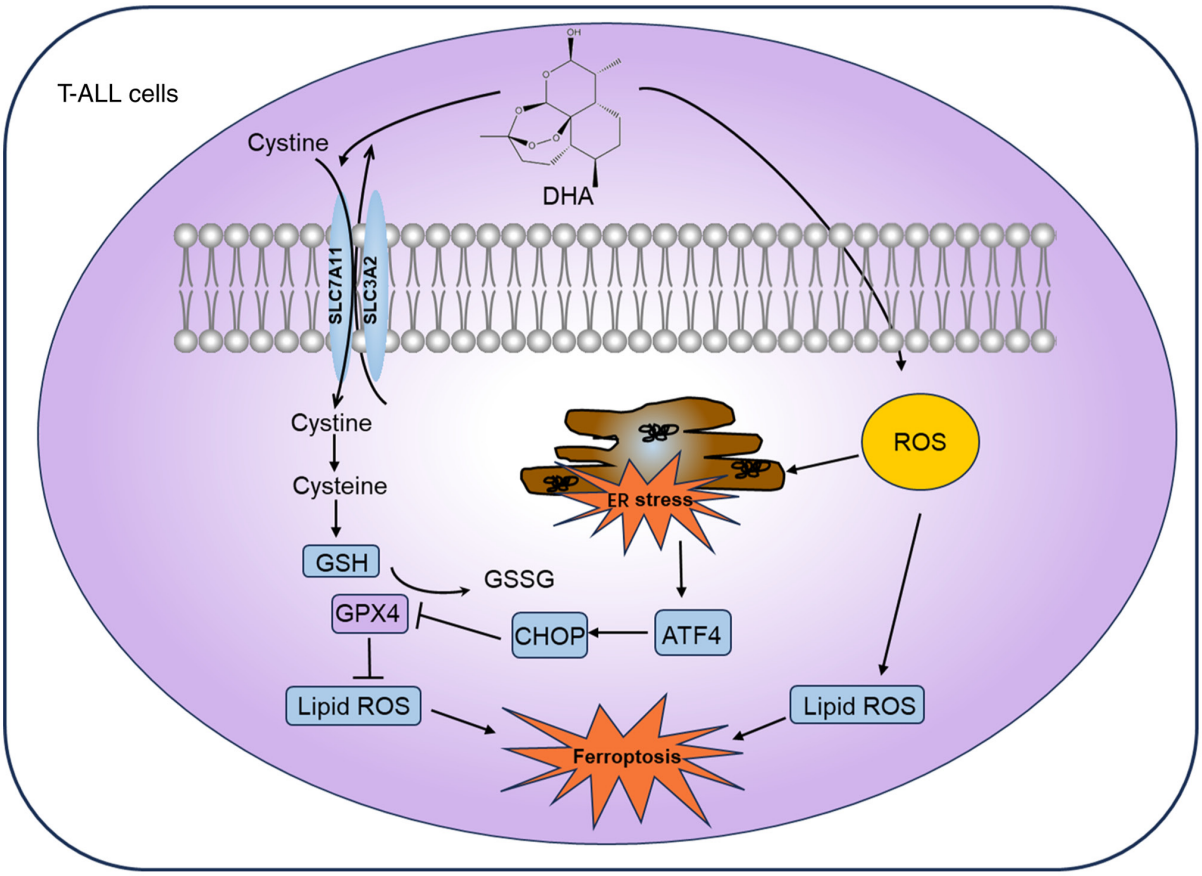

Figure 6. Illustration of the mechanism of DHA inhibiting T-ALL cell viability, inducing ferroptosis by modulating the SLC7A11-GPX4 signaling pathway and provoking ER stress. DHA, dihydroartemisinin; ER, endoplasmic reticulum; GPX4, GSH peroxidase 4; GSH, glutathione; ROS, reactive oxygen species; T-ALL, T-cell acute lymphoblastic leukemia.

In addition to its well-known anti-malarial applications, DHA is currently being evaluated for its potential to treat various types of cancer because of its high potency, low toxicity and short half-life (28), as well as its documented safety in patients with malaria. In the present study, the anti-leukemic effects of DHA were assessed in T-ALL cells. Initially, through the CCK-8 assay, it was demonstrated that DHA inhibited the viability of T-ALL cells, accompanied by a minor impact on normal human PBMCs. Cell cycle arrest is considered a key element in the antitumor activity of artemisinin derivatives (29). Consistent with the findings of Jin *et al* (30), it was observed that DHA induced cell cycle arrest at S phase and G_2/M phase, thereby inhibiting the viability of T-ALL cells. Apoptosis has been regarded as the primary form of cell death (31,32). The present study observed that, regardless of the concentration of DHA employed, dead cells were predominantly clustered in the right upper quadrant (Annexin V- and PI-positive) indicating late apoptotic cells. In addition, ROS accumulation was present in DHA-induced T-ALL cells. These findings suggested that, apart from apoptosis, there are other types of cell death induced by DHA in T-ALL cells.

Ferroptosis is a form of cell death that is dependent on ROS (33). The role of DHA in inducing ferroptosis in cancer cells was first reported in head and neck cancer cells (34), followed by acute myeloid leukemia cells (35). Ferroptosis is mainly associated with iron accumulation and lipid peroxidation (36). In the present study, the increased levels of the lipid peroxidation marker MDA and the decreased levels of GSH in the cells indicated a pronounced induction of ferroptosis in DHA-treated T-ALL cells. To further assess the contribution of ferroptosis to the anti-leukemic effects of DHA, Fer-1 was employed to rescue cellular viability. Fer-1 is a ferroptosis inhibitor, extensively utilized both *in vitro* and *in vivo* (37,38). Functioning as an antioxidant, the efficacy of Fer-1 in the inhibition of ferroptosis is primarily dependent on its suppression of lipid peroxidation (39). The results of the present study indicated that the co-treatment with DHA and Fer-1 exhibited a rescuing effect. It was observed that Fer-1 treatment significantly attenuated the function of DHA in decreasing the viability of T-ALL cells, and the proportion of late apoptotic or dead cells in the right upper quadrant of flow cytometry plots was decreased. Notably, Fer-1 treatment reduced the levels of ROS and MDA in the DHA group, while increasing the GSH levels. This may be related to the inhibition of lipid peroxidation by Fer-1; however, the underlying mechanisms still require further research.

Recently, ferroptosis has been recognized as an adaptive trait contributing to cancer cell destruction (40). Lipid ROS accumulation is a critical factor in triggering ferroptosis (41). Inactivation of the cellular antioxidant system is an important route leading to ROS generation. SLC7A11 and GPX4 are considered central regulatory elements

in ferroptosis, with GPX4 acting as the primary defensive enzyme against ferroptosis. The deficiency of GSH inhibits GPX4 activity, thereby promoting ferroptosis (42). In addition, it has been shown that system Xc^- transports cystine from the extracellular space into the intracellular space, promptly converting it to cysteine, thus furnishing the requisite materials for GSH synthesis. Inhibition of the system Xc^- can impede cysteine uptake, leading to decreased GSH levels and, consequently, insufficient GPX4 capacity to eliminate lipid ROS, ultimately inducing cell death (43). In the present study, DHA treatment reduced the expression levels of SLC7A11 and GPX4 in T-ALL cells. Furthermore, administration of Fer-1 increased the protein expression levels of SLC7A11 and GPX4 in Jurkat and Molt-4 cells. These findings suggested that ferroptosis serves a pivotal role in DHA-mediated inhibition of T-ALL, and the ferroptosis induced by DHA may be achieved through the inhibition of system Xc^-.

Excessive ROS is a crucial stimulating factor in the ER stress response. Lipid accumulation and oxidation are associated with disturbances in ER protein homeostasis, known as ER stress (44). Disturbances in ER homeostasis involve a series of stress response signaling pathways, collectively called the unfolded protein response (UPR). Although the UPR is an adaptive protective mechanism, in the presence of unresolvable ER stress, activation of ER stress by the UPR mediates cell death in tumor cells along with the ER stress prolongation and accumulation (45). ER stress has been reported to be a regulator of the progression of ferroptosis and one of the mechanisms by which DHA exerts its antitumor effects (10). A previous study reported that DHA kills protoscoleces through ER stress and the CHOP pathway (46). Dixon *et al* (22) demonstrated that erastin induces ferroptosis in various cellular environments by specifically inhibiting system Xc^-, and that small molecule inhibitors of system Xc^- trigger ER stress via the UPR. As an emerging inducer of ferroptosis, the present study observed that DHA can activate the ATF4-CHOP signaling pathway and induce ER stress in Jurkat and Molt-4 cells, leading to ferroptosis. Administration of Fer-1 decreased the protein expression levels of ATF4 and CHOP in Jurkat and Molt-4 cells. A previous study has shown that ATF4 protects against ferroptosis due to its ability to activate xCT transcription (47). It transcriptionally regulates membrane transporter proteins and enzymes required for GSH biosynthesis in cancer cells involved in chemoresistance (48). Nevertheless, ER stress has been shown to promote HMOX1-mediated ferroptosis caused by BAY11-7085, a IκBα inhibitor (49). A previous study evaluating the effects of artesunate on Burkitt lymphoma cells supported the findings of the present study (50).

The present study showed that DHA may activate ATF4/CHOP-mediated ER stress, which may be related to antioxidant system disturbances and excessive ROS accumulation. The upregulation of ATF4 and CHOP may lead to the degradation of GSH, thereby inducing ferroptosis. However, the current results do not exclude the regulatory role of other types of ROS, such as the increased ROS mediated by iron accumulation in the Fenton reaction, on DHA-induced ferroptosis in T-ALL cells. Further study is required to better understand the role of the ER stress-xCT axis in DHA-induced ferroptosis in T-ALL cells. Given the potential interconnection between ER stress and ferroptosis, a limitation of the present study lies in the need for deeper exploration to comprehensively grasp the intricate mechanisms underlying ferroptosis and the supplementary impacts elicited by DHA in the treatment of T-ALL. Our future studies would benefit from a combined approach that leverages both flow cytometry and molecular assays to provide a more complete understanding of the apoptotic mechanism induced by DHA in T-ALL cells. Additionally, the absence of *in vivo* animal experiments constitutes another constraint of the present study.

In conclusion, the results of the present study demonstrated that DHA may induce ferroptosis in different types of T-ALL cells and elicit a significant ER stress response in tumor cells. These findings may improve understanding of the antitumor potential of DHA and provide novel insights for the development of drugs for the treatment of T-ALL.

Acknowledgements

The authors would like to thank Professor Ying Song (Weifang Medical University) for critically reading the manuscript, and Dr Linda Hu (Upstate Medical University, New York, NY, USA) for critically reading and language editing the manuscript.

Funding

The present study was supported by the Shandong Provincial Natural Science Foundation of China (grant nos. ZR2020QH096 and ZR2020KC016).

Availability of data and materials

The data generated in the present study may be requested from the corresponding author.

Authors' contributions

NT and XL designed and performed experiments, analyzed the data and wrote the manuscript. YL, HW and YZ helped perform specific experiments and data analysis. HW and ZH designed and supervised the project, acquired funding and revised the manuscript. YL and HW confirm the authenticity of all the raw data. All authors have read and approved the final version of the manuscript.

Ethics approval and consent to participate

This present study was reviewed and approved by the Ethics Committee of the Affiliated Hospital of Weifang Medical University (approval no. wfmc-2023-ky-042). The participants provided their written informed consent to participate in this study.

Patient consent for publication

Not applicable.

Competing interests

The authors declare that they have no competing interests.

References

1. Belver L and Ferrando A: The genetics and mechanisms of T cell acute lymphoblastic leukaemia. Nat Rev Cancer 16: 494-507, 2016.
2. Vadillo E, Dorantes-Acosta E, Pelayo R and Schnoor M: T cell acute lymphoblastic leukemia (T-ALL): New insights into the cellular origins and infiltration mechanisms common and unique among hematologic malignancies. Blood Rev 32: 36-51, 2018.
3. Raetz EA and Teachey DT: T-cell acute lymphoblastic leukemia. Hematology Am Soc Hematol Educ Program 2016: 580-588, 2016.
4. Newman DJ, Cragg GM and Snader KM: Natural products as sources of new drugs over the period 1981-2002. J Nat Prod 66: 1022-1037, 2003.
5. Neill US: From branch to bedside: Youyou Tu is awarded the 2011 Lasker~DeBakey Clinical Medical Research Award for discovering artemisinin as a treatment for malaria. J Clin Invest 121: 3768-3773, 2011.
6. Cheong DHJ, Tan DWS, Wong FWS and Tran T: Anti-malarial drug, artemisinin and its derivatives for the treatment of respiratory diseases. Pharmacol Res 158: 104901, 2020.
7. Lemke D, Pledl HW, Zorn M, Jugold M, Green E, Blaes J, Löw S, Hertenstein A, Ott M, Sahm F, *et al*: Slowing down glioblastoma progression in mice by running or the anti-malarial drug dihydroartemisinin? Induction of oxidative stress in murine glioblastoma therapy. Oncotarget 7: 56713-56725, 2016.
8. Zhang CZ, Zhang H, Yun J, Chen GG and Lai PBS: Dihydroartemisinin exhibits antitumor activity toward hepatocellular carcinoma in vitro and in vivo. Biochem Pharmacol 83: 1278-1289, 2012.
9. Li Y, Zhou X, Liu J, Gao N, Yang R, Wang Q, Ji J, Ma L and He Q: Dihydroartemisinin inhibits the tumorigenesis and metastasis of breast cancer via downregulating CIZ1 expression associated with TGF-β1 signaling. Life Sci 248: 117454, 2020.
10. Dai X, Zhang X, Chen W, Chen Y, Zhang Q, Mo S and Lu J: Dihydroartemisinin: A potential natural Anti-Cancer drug. Int J Biol Sci 17: 603-622, 2021.
11. Li S, Huang P, Gan J, Ling X, Du X, Liao Y, Li L, Meng Y, Li Y and Bai Y: Dihydroartemisinin represses esophageal cancer glycolysis by down-regulating pyruvate kinase M2. Eur J Pharmacol 854: 232-239, 2019.
12. Wang T, Luo R, Li W, Yan H, Xie S, Xiao W, Wang Y, Chen B, Bai P and Xing J: Dihydroartemisinin suppresses bladder cancer cell invasion and migration by regulating KDM3A and p21. J Cancer 11: 1115-1124, 2020.
13. Sun WD, Yu XX, An YH, Wang X, Wang Y and Tong XM: Dihydroartemisinin induces apoptosis of human acute T lymphocytic leukemia cells by activating oxidative stress. Zhongguo Shi Yan Xue Ye Xue Za Zhi 28: 753-757, 2020 (In Chinese).
14. Wong KH, Yang D, Chen S, He C and Chen M: Development of nanoscale drug delivery systems of dihydroartemisinin for cancer therapy: A review. Asian J Pharm Sci 17: 475-490, 2022.
15. Shi H, Xiong L, Yan G, Du S, Liu J and Shi Y: Susceptibility of cervical cancer to dihydroartemisinin-induced ferritinophagy-dependent ferroptosis. Front Mol Biosci 10: 1156062, 2023.
16. Du J, Wang X, Li Y, Ren X, Zhou Y, Hu W, Zhou C, Jing Q, Yang C, Wang L, *et al*: DHA exhibits synergistic therapeutic efficacy with cisplatin to induce ferroptosis in pancreatic ductal adenocarcinoma via modulation of iron metabolism. Cell Death Dis 12: 705, 2021.
17. Cao JY and Dixon SJ: Mechanisms of ferroptosis. Cell Mol Life Sci 73: 2195-2209, 2016.
18. Tu H, Tang LJ, Luo XJ, Ai KL and Peng J: Insights into the novel function of system Xc-in regulated cell death. Eur Rev Med Pharmacol Sci 25: 1650-1662, 2021.
19. Dixon SJ, Lemberg KM, Lamprecht MR, Skouta R, Zaitsev EM, Gleason CE, Patel DN, Bauer AJ, Cantley AM, Yang WS, *et al*: Ferroptosis: An iron-dependent form of non-apoptotic cell death. Cell 149: 1060-1072, 2012.
20. Patanè GT, Putaggio S, Tellone E, Barreca D, Ficarra S, Maffei C, Calderaro A and Laganà G: Ferroptosis: Emerging role in diseases and potential implication of bioactive compounds. Int J Mol Sci 24: 17279, 2023.
21. Qin Y, Qiao Y, Wang D, Tang C and Yan G: Ferritinophagy and ferroptosis in cardiovascular disease: Mechanisms and potential applications. Biomed Pharmacother 141: 111872, 2021.
22. Dixon SJ, Patel DN, Welsch M, Skouta R, Lee ED, Hayano M, Thomas AG, Gleason CE, Tatonetti NP, Slusher BS, *et al*: Pharmacological inhibition of Cystine-glutamate exchange induces endoplasmic reticulum stress and ferroptosis. Elife 3: e02523, 2014.
23. Livak KJ and Schmittgen TD: Analysis of relative gene expression data using real-time quantitative PCR and the 2(-Delta Delta C(T)) method. Methods 25: 402-408, 2001.
24. Ursini F, Maiorino M, Valente M, Ferri L and Gregolin C: Purification from pig liver of a protein which protects liposomes and biomembranes from peroxidative degradation and exhibits glutathione peroxidase activity on phosphatidylcholine hydroperoxides. Biochim Biophys Acta 710: 197-211, 1982.
25. Miotto G, Rossetto M, Di Paolo ML, Orian L, Venerando R, Roveri A, Vučković AM, Bosello Travain V, Zaccarin M, Zennaro L, *et al*: Insight into the mechanism of ferroptosis inhibition by ferrostatin-1. Redox Biol 28: 101328, 2020.
26. Boelens J, Lust S, Offner F, Bracke ME and Vanhoecke BW: Review. The endoplasmic reticulum: A target for new anti-cancer drugs. In Vivo 21: 215-226, 2007.
27. Zhu S, Zhang Q, Sun X, Zeh HJ III, Lotze MT, Kang R and Tang D: HSPA5 regulates ferroptotic cell death in cancer cells. Cancer Res 77: 2064-2077, 2017.
28. Dai X, Zhang X, Chen W, Chen Y, Zhang Q, Mo S and Lu J: Dihydroartemisinin: A potential natural anticancer drug. Int J Biol Sci 17: 603, 2021.
29. Kiani BH, Kayani WK, Khayam AU, Dilshad E, Ismail H and Mirza B: Artemisinin and its derivatives: A promising cancer therapy. Mol Biol Rep 47: 6321-6336, 2020.
30. Jin H, Jiang AY, Wang H, Cao Y, Wu Y and Jiang XF: Dihydroartemisinin and gefitinib synergistically inhibit NSCLC cell growth and promote apoptosis via the Akt/mTOR/STAT3 pathway. Mol Med Rep 16: 3475-3481, 2017.
31. Ketelut-Carneiro N and Fitzgerald KA: Apoptosis, pyroptosis, and Necroptosis-Oh my! the many ways a cell can die. J Mol Biol 434: 167378, 2022.
32. Hänggi K and Ruffell B: Cell death, therapeutics, and the immune response in cancer. Trends Cancer 9: 381-396, 2023.
33. Tang D, Chen X, Kang R and Kroemer G: Ferroptosis: Molecular mechanisms and health implications. Cell Res 31: 107-125, 2021.
34. Lin R, Zhang Z, Chen L, Zhou Y, Zou P, Feng C, Wang L and Liang G: Dihydroartemisinin (DHA) induces ferroptosis and causes cell cycle arrest in head and neck carcinoma cells. Cancer Lett 381: 165-175, 2016.
35. Du J, Wang T, Li Y, Zhou Y, Wang X, Yu X, Ren X, An Y, Wu Y, Sun W, *et al*: DHA inhibits proliferation and induces ferroptosis of leukemia cells through autophagy dependent degradation of ferritin. Free Radic Biol Med 131: 356-369, 2019.
36. Li J, Cao F, Yin HL, Huang ZJ, Lin ZT, Mao N, Sun B and Wang G: Ferroptosis: Past, present and future. Cell Death Dis 11: 88, 2020.
37. Lai K, Song C, Gao M, Deng Y, Lu Z, Li N and Geng Q: Uridine alleviates Sepsis-Induced acute lung injury by inhibiting ferroptosis of macrophage. Int J Mol Sci 24: 5093, 2023.
38. Liu GZ, Xu XW, Tao SH, Gao MJ and Hou ZH: HBx facilitates ferroptosis in acute liver failure via EZH2 mediated SLC7A11 suppression. J Biomed Sci 28: 67, 2021.
39. Miotto G, Rossetto M, Di Paolo ML, Orian L, Venerando R, Roveri A, Vučković AM, Bosello Travain V, Zaccarin M, Zennaro L, *et al*: Insight into the mechanism of ferroptosis inhibition by ferrostatin-1. Redox Biol 28: 101328, 2020.
40. Li L, Qiu C, Hou M, Wang X, Huang C, Zou J, Liu T and Qu J: Ferroptosis in ovarian cancer: A Novel therapeutic strategy. Front Oncol 11: 665945, 2021.
41. Cheung EC and Vousden KH: The role of ROS in tumour development and progression. Nat Rev Cancer 22: 280-297, 2022.
42. Seibt TM, Proneth B and Conrad M: Role of GPX4 in ferroptosis and its pharmacological implication. Free Radic Biol Med 133: 144-152, 2019.
43. Lee N, Carlisle AE, Peppers A, Park SJ, Doshi MB, Spears ME and Kim D: xCT-Driven expression of GPX4 determines sensitivity of breast cancer cells to ferroptosis inducers. Antioxidants (Basel) 10: 317, 2021.
44. Zhang Z, Zhang L, Zhou L, Lei Y, Zhang Y and Huang C: Redox signaling and unfolded protein response coordinate cell fate decisions under ER stress. Redox Biol 25: 101047, 2019.

45. Bhardwaj M, Leli NM, Koumenis C and Amaravadi RK: Regulation of autophagy by canonical and non-canonical ER stress responses. Semin Cancer Biol 66: 116-128, 2020.
46. Ma R, Qin W, Xie Y, Han Z, Li S, Jiang Y and Lv H: Dihydroartemisinin induces ER stress-dependent apoptosis of Echinococcus protoscoleces in vitro. Acta Biochim Biophys Sin (Shanghai) 52: 1140-1147, 2020.
47. Chen D, Fan Z, Rauh M, Buchfelder M, Eyupoglu IY and Savaskan N: ATF4 promotes angiogenesis and neuronal cell death and confers ferroptosis in a xCT-dependent manner. Oncogene 36: 5593-5608, 2017.
48. Chen D, Rauh M, Buchfelder M, Eyupoglu IY and Savaskan N: The oxide-metabolic driver ATF4 enhances temozolomide chemo-resistance in human gliomas. Oncotarget 8: 51164-51176, 2017.
49. Chang LC, Chiang SK, Chen SE, Yu YL, Chou RH and Chang WC: Heme oxygenase-1 mediates BAY 11-7085 induced ferroptosis. Cancer Lett 416: 124-137, 2018.
50. Wang N, Zeng GZ, Yin JL and Bian ZX: Artesunate activates the ATF4-CHOP-CHAC1 pathway and affects ferroptosis in Burkitt's Lymphoma. Biochem Biophys Res Commun 519: 533-539, 2019.